

Radio-Excess *IRAS* Galaxies: Low Power CSS/GPS Sources?

Catherine L. Drake^{1,2}, Peter J. McGregor¹, Geoffrey V. Bicknell¹
and Michael A. Dopita¹

¹Research School of Astronomy and Astrophysics, Australian National University,
Cotter Road, Weston, ACT 2611, Australia
cdrake@mso.anu.edu.au
peter@mso.anu.edu.au
geoff@mso.anu.edu.au
mad@mso.anu.edu.au

²Australia Telescope National Facility, PO Box 76, Epping, NSW 1710, Australia

Received 2002 August 6, accepted 2002 December 10

Abstract: Amongst our sample of radio-excess *IRAS* galaxies, we have identified compact steep spectrum radio sources that fall into the classes of CSS or GPS sources, but have not previously been identified as such. The sample includes objects that have radio powers as low as $\sim 10^{22}$ W Hz⁻¹. We suggest that these are low-power analogues of CSS and GPS sources, with weaker radio jets. These may be precursors to FR I radio galaxies or may ‘fade’ into radio-quiet galaxies.

Keywords: galaxies: active — infrared: galaxies — radio continuum: galaxies

1 Radio-Excess *IRAS* Galaxies

The term *radio-excess* is widely used to describe galaxies that have excess radio emission above that expected according to the correlation between far infrared (FIR) and radio flux observed for star-forming galaxies and radio-quiet active galactic nuclei (AGN). The description covers radio-loud objects as well as objects with intermediate radio/FIR flux ratios. We have selected a sample of radio-excess *IRAS* galaxies for the purpose of studying these intermediate-excess objects that fall between the traditional classes of radio-loud and radio-quiet (C. L. Drake et al., in preparation). This radio-excess sample was selected from a larger sample of radio/FIR objects identified by cross-correlating the *IRAS* FSC (60 μ m sources: Moshir et al. 1992) with the PMN 5 GHz catalogue (Griffith & Wright 1993). Figure 1(a) shows the FIR/radio luminosity diagram for the larger sample, highlighting the radio-excess objects.

We find that many ($\sim 40\%$) of the radio sources in our sample are compact and have steep spectral indices, that is, they fit the definition of compact steep spectrum (CSS) or gigahertz peaked spectrum (GPS) radio sources.¹ Figure 1(b) highlights these CSS objects as well as the four known CSS/GPS sources in the sample. The objects cover a range in radio power as high as CSS/GPS sources but also extend to lower radio powers of $\sim 10^{22}$ W Hz⁻¹. These objects have upper limits on their sizes of ≤ 15 kpc and spectral indices at GHz frequencies of $\alpha < -0.5$ ($S_\nu \propto \nu^\alpha$). A few of the objects are resolved on arcsecond scales at radio wavelengths. These have symmetric double or triple morphologies, similar to CSS/GPS galaxies

(see Figure 2). The measured limits on their sizes and turnover frequencies place these objects on or near the observed turnover frequency–projected linear size relation for CSS/GPS sources (Figure 3). We suggest, from their sizes, spectral indices, and morphologies, that these are low-power CSS/GPS sources.

2 Weak Radio Jets?

The spectral energy distributions of the compact radio-excess sources show steep or peaked radio spectra (Figure 4). A turnover in the radio spectrum at ~ 1 GHz is seen in a few objects and a break in the spectrum at higher frequencies is seen in others. However, most sources show only a very steep spectrum with slope $\alpha \sim -1.0$. This slope may be attributed to synchrotron cooling and implies an upper limit on the break frequency that may be used to estimate the age of the radio source. We use the object F15306-0832 (shown in Figure 2) as an example: assuming minimum energy conditions, the magnetic field in the lobes is 44–71 μ G. Combined with the lower limit on the break frequency of 8.64 GHz (Figure 5), this gives a synchrotron cooling timescale of $\leq 1-2 \times 10^6$ years. This implies the source is young, but is at least an order of magnitude older than the ages of typical CSS and GPS sources, determined using observed break frequencies (Murgia et al. 1999) and hot spot advance speeds (Owsianik & Conway 1998; Owsianik, Conway, & Polatidis 1998, 1999). If we assume the synchrotron timescale to be approximately the age of the radio source, the projected linear size of 1.9 kpc implies an advance speed of the lobes of $\leq 500-1000$ km s⁻¹. This is significantly slower than the advance speeds of $\sim 0.1-0.2 c$ inferred for CSS/GPS sources (Owsianik & Conway 1998; Owsianik et al. 1998, 1999). We suggest that these low-power CSS/GPS sources have weaker radio jets that cause the lobes to advance more

¹This fraction is larger than in other radio-selected samples, but this is probably not significant as selection effects may have excluded extended objects from our sample.

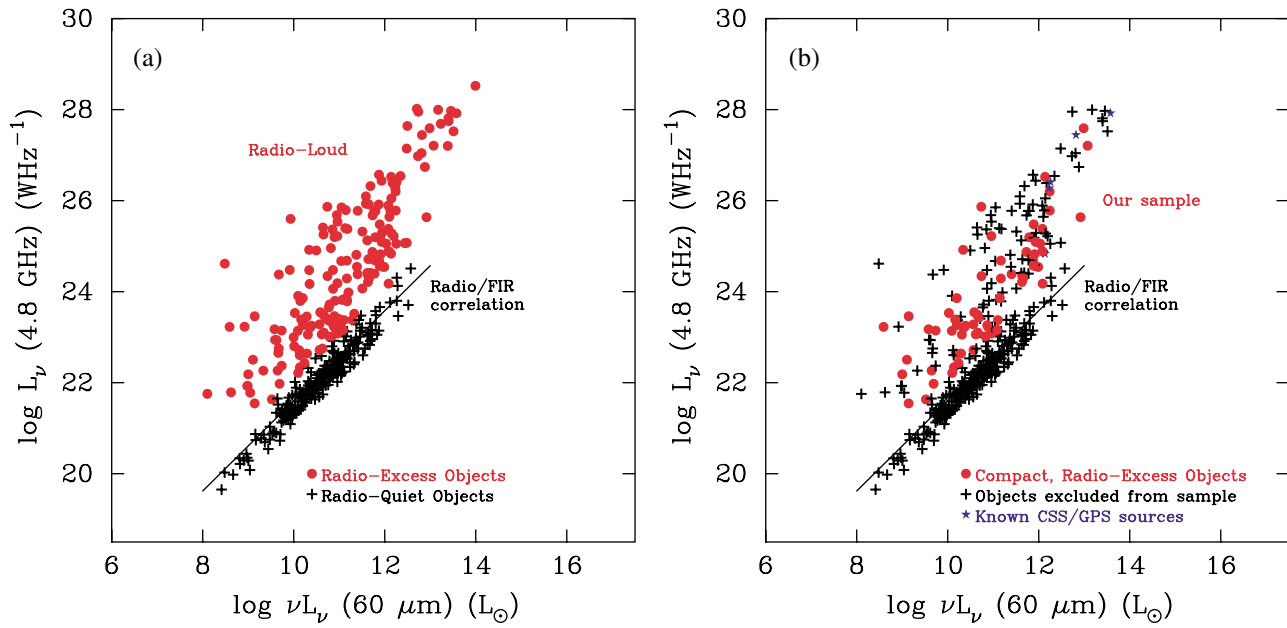


Figure 1 FIR/radio luminosity diagrams. (a) All radio-excess objects are shown as bullets, to highlight their location above the FIR/radio correlation for radio-quiet objects (crosses). (b) Only compact radio sources (projected linear size < 15 kpc) with steep or inverted spectral index ($\alpha < -0.5$ or $\alpha > 0.0$; $S_\nu \propto \nu^\alpha$) are shown as bullets. Four known CSS/GPS sources in the sample are indicated by stars. Extended radio sources (projected linear size > 15 kpc), compact flat spectrum sources and known blazars are not of relevance to this paper and are shown, along with radio-quiet objects, as crosses. Objects for which the radio size and/or the spectral index is unknown are omitted.

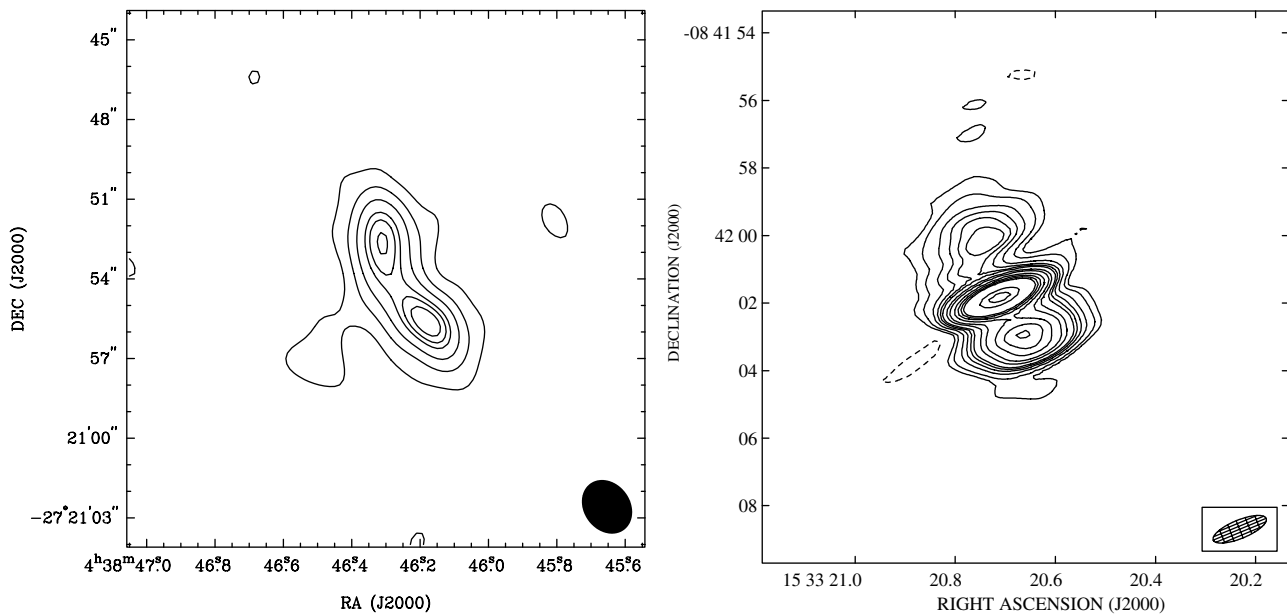


Figure 2 Radio contour maps of the resolved sources F04367-2726 and F15306-0832. F04367-2726 was observed with the ATCA 6A configuration at 8.6 GHz; the contours are 10, 30, 50, 70, 80, and 90% of the peak, 8.4 mJy/beam. F15306-0832 was observed with the VLA BnA configuration at 4.8 GHz; the contours are -0.5 , 0.5 , 1 , 2 , 3 , 4 , 5 , 7.5 , 10 , 15 , 20 , 25 , 30 , 70 , and 90% of the peak, 40 mJy/beam.

slowly than typical CSS/GPS sources, so they are older despite being similar in size. The jet energy flux may be estimated by assuming it is proportional to the radio power and taking a typical ratio of power to jet energy flux ratio of 10^{-12} (Bicknell et al. 1998). An observed radio power of 10^{23} W Hz^{-1} implies a jet energy flux $\sim 10^{42}$ erg s^{-1} . This is several orders of magnitude weaker than the jet energy

fluxes of $10^{46.5}$ erg s^{-1} inferred for powerful CSS/GPS sources (Bicknell, Saxton, & Sutherland 2003).

Broad $[\text{O III}] \lambda 5007 \text{ \AA}$ line emission suggests strong interaction between the radio source and host galaxy interstellar medium (ISM). Figure 6 shows the distribution of $[\text{O III}] \lambda 5007 \text{ \AA}$ linewidths for the compact radio-excess objects compared with other classes of objects, including

CSS sources (Gelderman & Whittle 1997). The broad linewidths in the radio-excess *IRAS* galaxies are similar to those in CSS sources, consistent with strong interaction between the embedded radio source and host galaxy ISM, and presumably relating to the driving of radiative

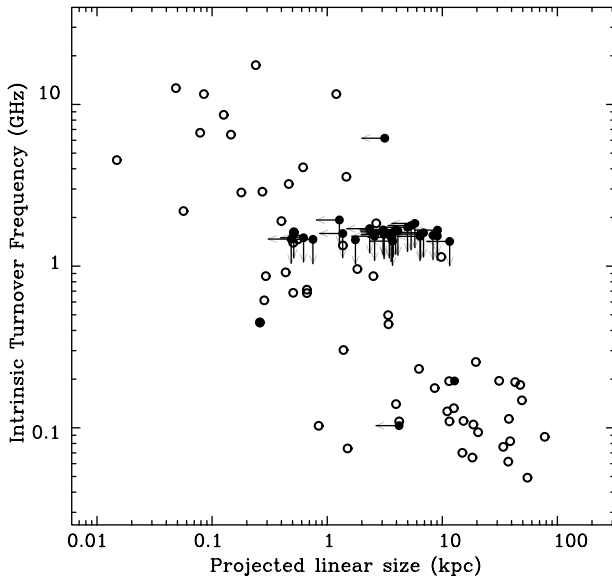


Figure 3 Turnover frequency–size plot showing the location of radio-excess *IRAS* galaxies (filled circles) relative to powerful CSS/GPS sources (open circles: O’Dea 1998).

shocks into the ambient gas. For those objects with measured [O III] λ 5007 Å line emission, the line luminosity in the radio-excess *IRAS* objects is comparable with that in CSS/GPS sources, $L_{[\text{O III}]} = 10^{41} - 10^{44} \text{ erg s}^{-1}$, but the radio power is a factor of 10–100 lower ($P_{5 \text{ GHz}} = 10^{24} - 10^{26} \text{ W Hz}^{-1}$ for the radio-excess *IRAS* objects compared with $P_{5 \text{ GHz}} = 10^{26} - 10^{28} \text{ W Hz}^{-1}$ for the CSS sources). Figure 7 shows histograms comparing the ratio of [O III] λ 5007 Å luminosity to radio power for CSS sources and the compact radio-excess objects. The radio-excess objects have higher ratios of [O III] λ 5007 Å line luminosity to radio power than the more powerful CSS sources. In the context of shock models used to describe the production of [O III] line emission by expanding radio lobes (Bicknell, Dopita, & O’Dea 1997; de Vries et al. 1999; Bicknell et al. 2003), there are a number of possible reasons for this. In the more powerful CSS/GPS sources, it is possible that the bow shock at the front of the lobe is too fast and so only the shocks at the sides of the lobes are radiative; the bow shock in the weaker sources may be radiative around the entire lobe. Furthermore, a condition for the bow shock to produce optical emission depends on the bow shock velocity and the density contrast between the diffuse ISM and dense clouds embedded in it (Bicknell et al. 2003). A weaker bow shock will be radiative for a larger range of cloud/ISM density contrasts and thus in the weaker objects more of the shocked medium may be radiative.

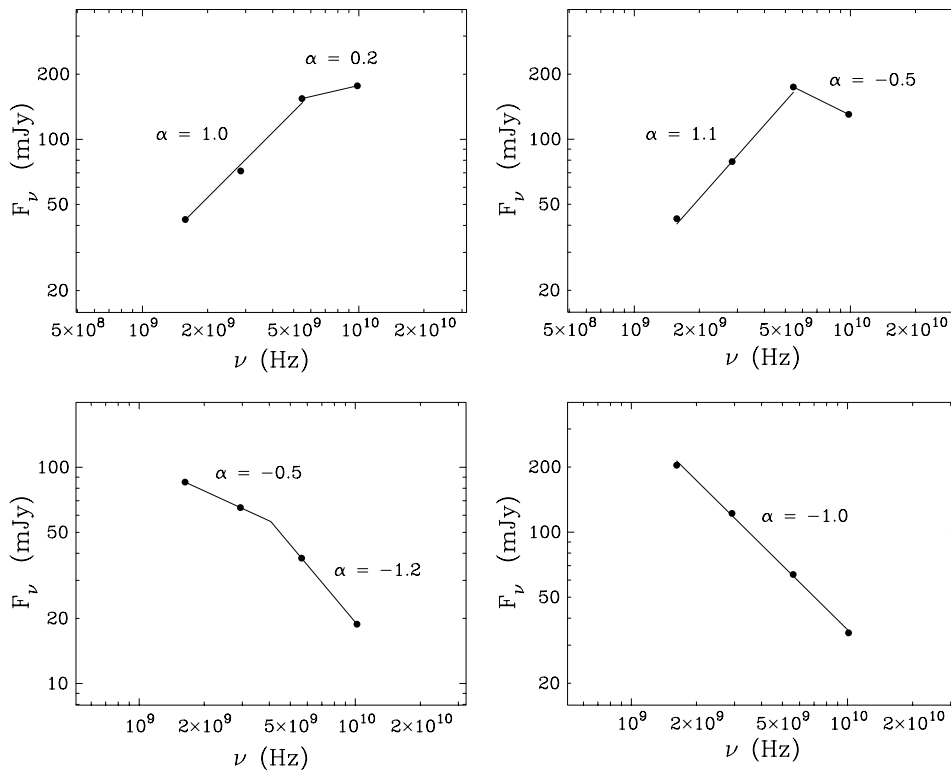


Figure 4 Typical spectral energy distributions of the compact radio-excess objects. Fluxes were measured with the ATCA or the VLA. Not all flux measurements were simultaneous, but little is known about the variability of these sources, so we neglect the effects of variability in this discussion.

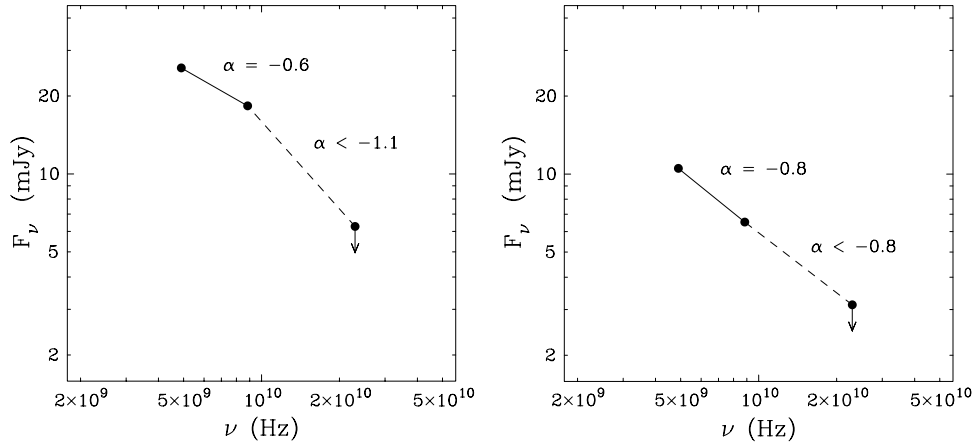


Figure 5 Spectral energy distributions of the south (left) and north (right) lobes of F15306-0832.

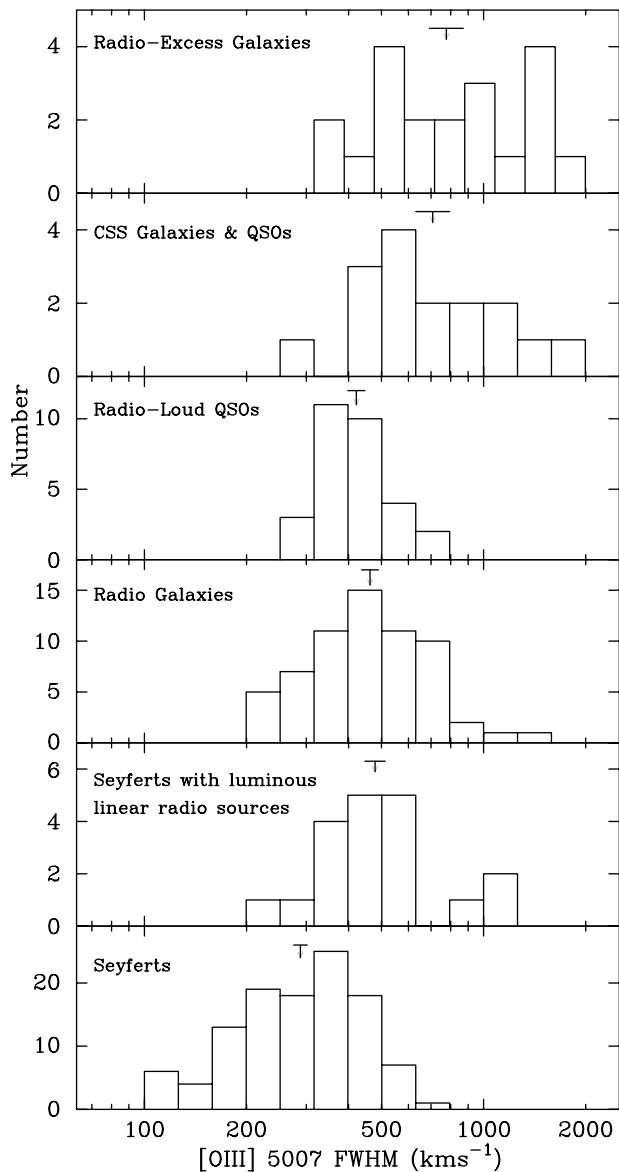


Figure 6 Histograms showing the distribution of [O III] λ 5007 Å linewidths for radio-excess *IRAS* objects (top panel) and comparison objects (Gelderman & Whittle 1997). The logarithmic median velocity is indicated for each histogram.

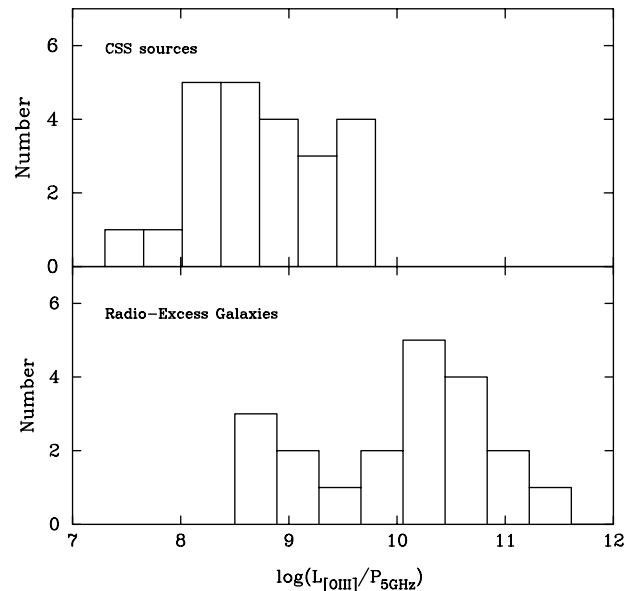


Figure 7 Histograms of the ratio $\log(L_{[\text{OIII}]} / P_{5\text{GHz}})$ for the radio-excess *IRAS* objects and CSS sources (Gelderman & Whittle 1994).

3 Hosts and Evolution

The compact radio-excess objects in our sample appear to be post-starburst AGN associated with bright merging host galaxies. Figure 8 shows typical host galaxy images and example post-starburst optical spectra. The spectra show emission lines as well as strong continuum and young stellar absorption. If the merging activity is associated with triggering or fuelling the radio source, this further supports the argument that these are relatively young radio sources. We expect the radio source to evolve on a shorter timescale than the FIR or optical source, and so objects should move approximately vertically on Figure 1 as they evolve. According to models of radio source evolution (e.g. Begelman 1996; Bicknell et al. 1997), we might expect a source to decrease in luminosity by a factor of 100 as it expands from a size of 10 kpc

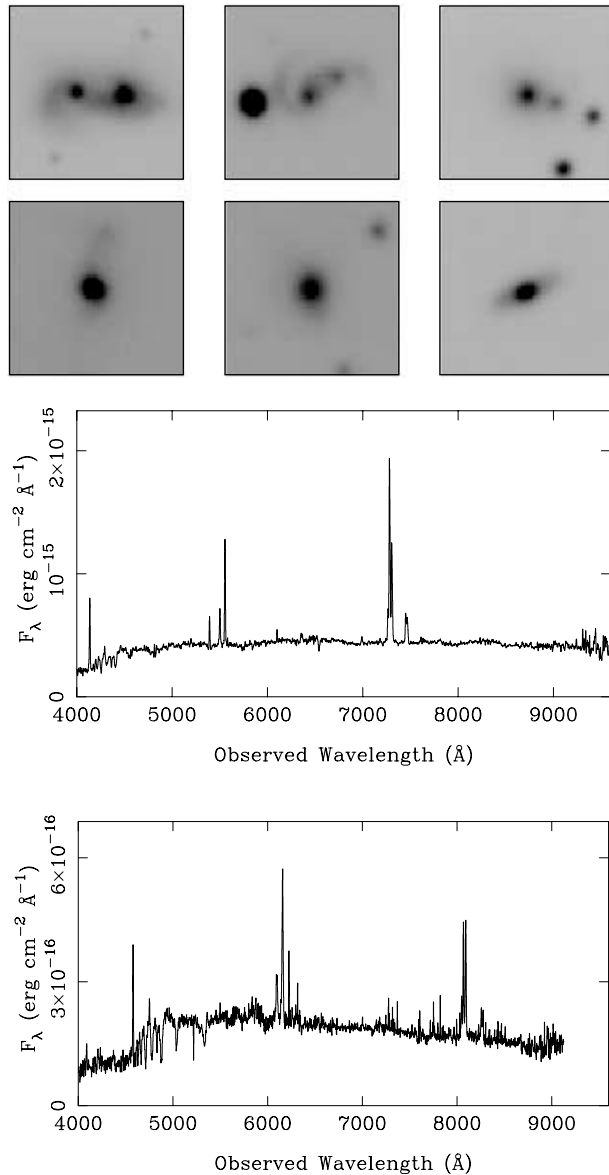


Figure 8 Host galaxy images and post-starburst AGN spectra.

to 100 kpc. Consequently an object initially with a radio power of $10^{24} \text{ W Hz}^{-1}$ will decrease to $10^{23} \text{ W Hz}^{-1}$ and may appear as an FR I. However, an object of $10^{23} \text{ W Hz}^{-1}$ will decrease to $10^{22} \text{ W Hz}^{-1}$ and so may move onto the FIR/radio correlation and become a radio-quiet galaxy.

4 Summary

We have identified candidate low power CSS/GPS sources amongst radio-excess *IRAS* galaxies. We suggest that these

objects have weaker radio jets than typical CSS/GPS sources, which accounts for their weaker observed radio power. This conclusion is supported by the observed steep radio spectrum and inferred age of the radio source in one particular case. Strong, broad $[\text{O III}] \lambda 5007 \text{ \AA}$ line emission suggests strong interaction between the radio source and the host ISM and high ratios of $[\text{O III}] \lambda 5007 \text{ \AA}$ line luminosity to radio power are interpreted as resulting from radiative shocks produced by the relatively weak radio jets. These objects may be the precursors to FR I radio galaxies, or may evolve into radio-quiet galaxies. There is no evidence in the FIR data that the hosts of the compact radio-excess sources are different from those of extended radio sources. A study of the optical host galaxies of the radio-excess sources is currently being undertaken, to compare these objects with extended radio galaxies and radio-quiet objects.

Acknowledgments

CD gratefully acknowledges the support of an Alex Rodgers Travelling Scholarship, which made it possible for her to attend the workshop. This research has made use of data obtained with the Very Large Array and the Australia Telescope National Facility. The VLA is operated by the National Radio Astronomy Observatory, which is a facility of the National Science Foundation operated under cooperative agreement by Associated Universities, Inc. The Australia Telescope is funded by the Commonwealth of Australia for operation as a National Facility managed by CSIRO.

References

- Begelman, M. C. 1996, in *Cygnus A — Study of a Radio Galaxy*, eds C. L. Carilli & D. E. Harris, (Cambridge: Cambridge University Press), 209
- Bicknell, G. V., Dopita, M. A., & O’Dea, C. P. 1997, *ApJ*, 485, 112
- Bicknell, G. V., Saxton, C. J., & Sutherland, R. S. 2003, *PASA*, 20, in press
- Bicknell, G. V., Dopita, M. A., Tsvetanov, Z. I., & Sutherland, R. S. 1998, *ApJ*, 495, 680
- de Vries, W. H., O’Dea, C. P., Baum, S. A., & Barthel, P. D. 1999, *ApJ*, 526, 27
- Gelderman, R., & Whittle, M. 1994, *ApJS*, 91, 491
- Gelderman, R., & Whittle, M. 1997, preprint
- Griffith, M. R., & Wright, A. E. 1993, *AJ*, 105, 1666
- Moshir, M., et al. 1992, Explanatory Supplement to the *IRAS* Faint Source Survey, Version 2, JPL D-10015 8/92 (Pasadena: JPL)
- Murgia, M., Fanti, C., Fanti, R., Gregorini, L., Klein, U., Mack, K.-H., & Vigotti, M. 1999, *A&A*, 345, 769
- O’Dea, C. P. 1998, *PASP*, 110, 493
- Owsianik, I., & Conway, J. E. 1998, *A&A*, 337, 69
- Owsianik, I., Conway, J. E., & Polatidis, A. G. 1998, *A&A*, 336, L37
- Owsianik, I., Conway, J. E., & Polatidis, A. G. 1999, *NewAR*, 43, 669